



Short communication

Gold nanoparticles-based biosensing of single nucleotide DNA mutations

Pazit Polak^{a,b,1}, Zeev Zalevsky^{a,b,*}, Orit Shefi^{a,b,**}^a Faculty of Engineering, Bar Ilan University, Ramat-Gan 52900, Israel^b The Bar-Ilan Institute of Nanotechnology and Advanced Materials, Bar Ilan University, Ramat-Gan 52900, Israel

ARTICLE INFO

Article history:

Received 25 March 2013

Accepted 8 April 2013

Available online xxx

Keywords:

DNA mutations

Gold nanoparticles

Biosensors

ABSTRACT

Detection of DNA mutations is critical for scientific research and diagnostic procedures. Here, we propose a novel interdisciplinary method for rapid and simple detection of DNA mutations. We show that heating a solution containing DNA and gold nanoparticles results in degradation of the DNA. Surprisingly, we found that the DNA can be protected against degradation, if an oligonucleotide that matches the DNA is added to the solution. Moreover, the level of degradation indicates the presence of mutations in the DNA. The method is sensitive enough to indicate even a single nucleotide difference, and has the potential to ultimately replace initial medical genetic tests. As proof of concept, we demonstrate a clear detection of two of the most common mutations leading to Cystic Fibrosis.

© 2013 Elsevier B.V. All rights reserved.

1. Introduction

Detection of DNA mutations is elementary practice for medical genetic tests as well as for scientific laboratory applications. Medical tests and screens relying on DNA mutation detection include routine preconception and prenatal genetic screens, and tests for disease predisposition. Traditional methods for mutation detection include sequencing, PCR, fluorescent in situ hybridization, restriction fragment length polymorphism, biosensors and microarrays [1–8]. However, not all methods are suitable for detection of any kind of mutation, and specifically for detection of point mutations.

Nanoparticles are used in biology and medicine [9–11]. Recent studies have demonstrated the use of nanoparticles for DNA mutation detection. These methods are based on nanoparticles that are attached to DNA molecules and change their properties in response to mutations. We study the interaction between DNA molecules and unbound nanoparticles. A previous study has reported that DNA attached to gold nanoparticles, that is heated for several hours, undergoes degradation [12]. Here we report that heating DNA in the presence of unbound nanoparticles results in rapid degradation. If an oligonucleotide that matches this DNA is added to the solution prior to heating, the degradation is slowed down considerably.

* Corresponding author at: Faculty of Engineering, Bar Ilan University, Ramat-Gan 52900, Israel. Tel.: +972 3 531 7055; fax: +972 3 738 4051.

** Corresponding author at: Faculty of Engineering, Bar Ilan University, Ramat-Gan 52900, Israel. Tel.: +972 3 531 7079; fax: +972 3 738 4051.

E-mail addresses: pazit.polak@biu.ac.il (P. Polak), zalevsz@biu.ac.il (Z. Zalevsky), orit.shefi@biu.ac.il (O. Shefi).

¹ Tel.: +973 3 531 7604; fax: +972 3 738 4051.

Remarkably, we discovered that the level of protection following the addition of an oligonucleotide with even one mismatch, significantly decreases. Thus, we propose a novel approach for detection of DNA mutations.

2. Results

We observed that heating a solution containing a DNA plasmid and gold nanoparticles results in degradation of the DNA plasmid in Fig. 1a, pUC19 DNA plasmid was incubated in the presence or absence of gold nanoparticles for 5 min, and then heated at 95 °C for 3 min. The mixture was allowed to cool at room temperature, followed by removal of the nanoparticles using a DNA cleanup kit. The DNA was visualized on an agarose gel. The result indicates that heating in the presence of nanoparticles causes the DNA to degrade (lane 1 vs. 2). Heating the DNA without nanoparticles does not cause the DNA to degrade (lane 3), indicating that the nanoparticles are essential for the degradation effect.

Next we observed that addition of an oligonucleotide that matches the DNA partially protects the DNA from degradation, while an oligonucleotide that does not match the DNA does not protect it (Fig. 1b). A mixture of DNA plasmid and gold nanoparticles were incubated as in Fig. 1a, with the addition of an oligonucleotide that fully matches the DNA (lanes 1 and 2) or an oligonucleotide that does not match the DNA (lane 3). Where indicated, the mixtures were then heated for 80 s. The mixtures were allowed to cool, nanoparticles were removed, and the DNA was visualized as in Fig. 1a. Clearly, the oligonucleotide that matches the DNA partly protects the DNA from degradation, whereas the oligonucleotide that does not match the DNA does not protect the DNA.

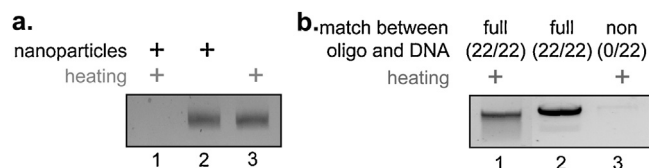


Fig. 1. Heating of a DNA plasmid in the presence of gold nanoparticles and oligonucleotides indicates the presence of DNA mutations. (a) A black "+" indicates that the samples contained gold nanoparticles. A gray "+" indicates that the samples were heated. b. The oligonucleotide that fully matches the DNA is 35, the oligonucleotide that does not match is 9 (see Section 4 for sequences). "+" Indicates that the samples were heated. An irrelevant lane was digitally removed between lanes 1 and 2 in this figure.

The protection from degradation is especially surprising since the oligonucleotides were only 22 bases in length, compared to the DNA plasmid which was 2686 base pairs long.

In light of our finding that the match between the oligonucleotide and the DNA is important for protection from degradation, we hypothesized that the level of degradation might be an indicator

of the level of mismatch between the oligonucleotide and DNA. We therefore compared the level of protection conferred on the DNA by a fully matching oligonucleotide vs. an oligonucleotide containing a mismatch (Fig. 2a). Again, heating of the DNA without oligonucleotides causes degradation of the DNA (lane 1), whereas unheated DNA remains intact (lane 4). As previously, an oligonucleotide that fully matches the DNA partly protects the DNA against degradation (lane 2). Confirming our hypothesis, we discovered that an oligonucleotide with one mismatch (lane 3) protects the DNA to a significantly lower extent compared to the oligonucleotide that fully matches the DNA. The difference was quantified and the band intensity of the oligonucleotide with partial match was found to be on average 26% lower compared to the oligonucleotide that fully matches the DNA (Fig. 2b). The different levels of protection conferred on the DNA by two oligonucleotides with only one different nucleotide between them, indicates that this system can be used to detect mutations.

We tested several time durations of heating, and noticed that the level of degradation of the DNA directly correlates to the time

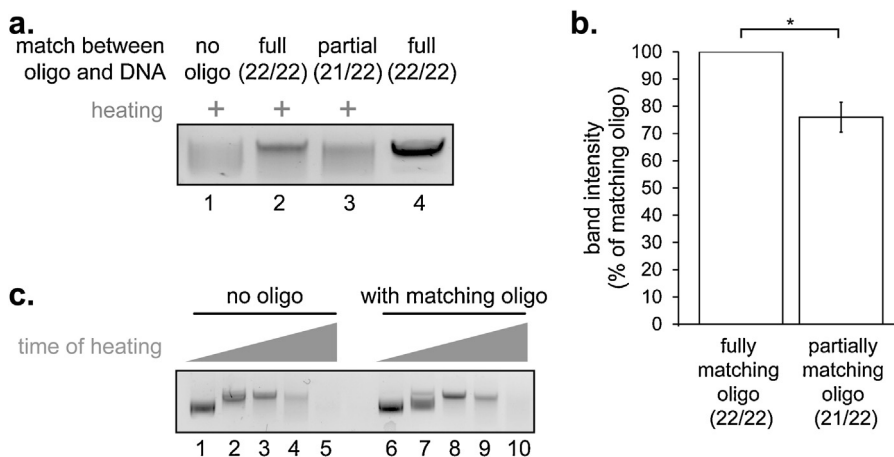


Fig. 2. (a) The oligonucleotide that fully matches the DNA is 35, the oligonucleotide with partial mismatch is 36. "+" Indicates that the samples were heated. An irrelevant lane was digitally removed between lanes 3 and 4 in this figure. (b) Densitometry of the difference between oligo 35 and 36. The graph shows an average of 7 independent experiments with S.E.M., p value is 0.0046. Oligo 35 is referred to as 100%. Densitometry was done using the imageJ software. (c) Time durations of heating were 0 for lanes 1 and 6; 30 s for lanes 2 and 7; 1 min for lanes 3 and 8; 2 min for lanes 4 and 9; and 3 min for lanes 5 and 10. The matching oligonucleotide is 35.

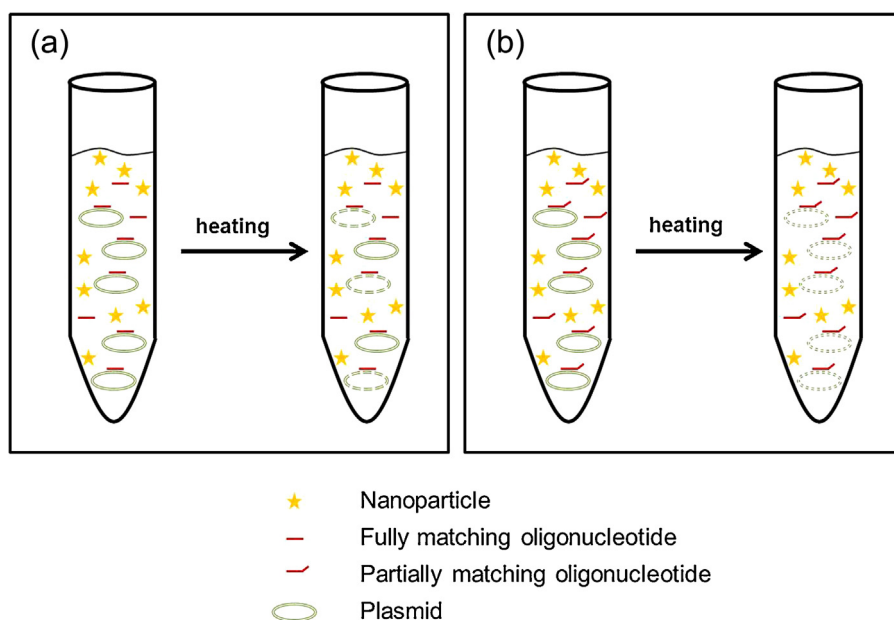


Fig. 3. Illustration of the method. (For interpretation of the references to color in the text, the reader is referred to the web version of the article.)

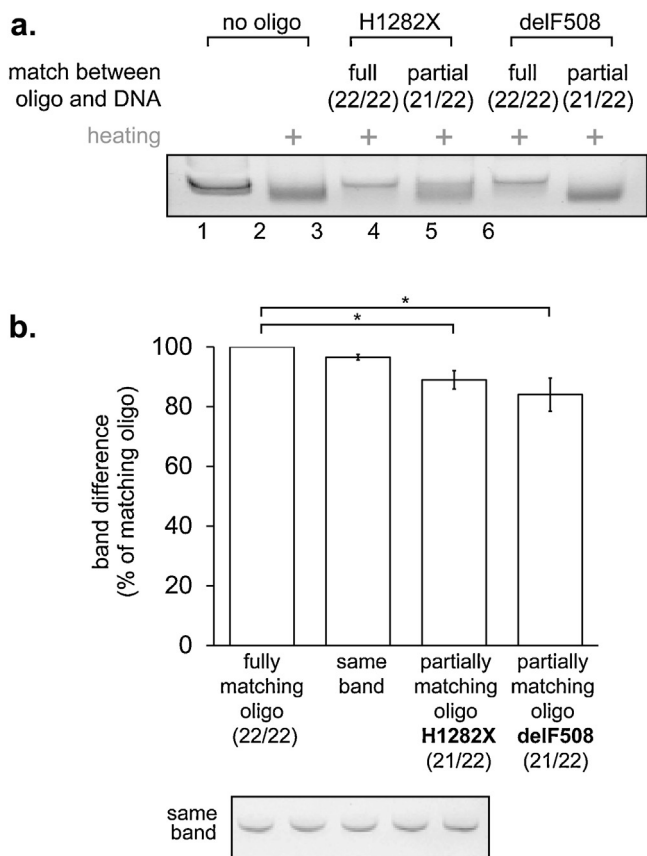


Fig. 4. The plasmid pCFmut was used for this figure. (a) Oligonucleotides: lane 3–107, lane 4–97 and lane 6–98. Irrelevant lanes were digitally removed between lanes 2 and 3, 4 and 5 in this figure. (b) Quantification of the difference between the mutated and WT oligonucleotides. The graph shows an average of 6 independent experiments with S.E.M., *p* value is 0.029 for mutation 1282, and 0.031 for mutation 508. The respective fully matching oligos are referred to as 100%.

of heating (Fig. 2c). Importantly, the protection conferred on the DNA by the oligonucleotide that fully matches, is evident only at the intermediate time points (compare lanes 3 with 8 and 4 with 9). Therefore, careful optimization of the heating time is required.

The procedure is illustrated in Fig. 3. In Fig. 3a we have an unmutated plasmid (green), and in Fig. 3b a mutated plasmid. The oligonucleotide (red) is identical in Fig. 3a and b, and fully matches the unmutated plasmid but not the mutated plasmid. After heating in the presence of nanoparticles (yellow), the oligo therefore protects the unmutated plasmid better than it protects the mutated plasmid, which is degraded to a higher degree compared to the unmutated plasmid.

In order to show that our method can be useful for diagnostic purposes, we chose two of the most common mutations that cause the disease Cystic Fibrosis, and successfully detected their presence (Fig. 4a). We generated a DNA plasmid, containing an insert with sequences spanning our two chosen mutations. The chosen mutations were delF508 and H1282X (see description of the pCFmut plasmid and mutations in Section 4). The presence of the mutations was successfully identified using our method (compare lanes 3 with 4 and 5 with 6). As seen in Fig. 2c, optimization of the heating time is required in order to observe the difference in protection level between the fully and partially matching oligos. For the detection of Cystic Fibrosis, this difference was most clear when using a relatively short heating time, which did not result in full degradation of the DNA. Although the difference in band shape is clearly visible by eye, we could not use regular densitometry for the detection of this difference. The difference in band histograms was

therefore quantified using an algorithm we developed specifically for this purpose: conventional discrimination between bands is performed only based on gray levels information and is performed over 1-D gray level distribution. Our phase space based processing converts the 1-D gray level information into 2-D textural distribution, allowing much higher discrimination (see Section 4 for further details). Analysis of our results using this algorithm showed that the oligonucleotides with one mismatch were 11% and 16% different compared to the oligonucleotides that fully match the DNA for mutations 1282 and 508, respectively (Fig. 4b). As a control for the quality of our algorithm, we ran the same DNA on several lanes in one gel, and quantified them expecting to find very minor differences if any. Indeed, the difference between the bands of the same untreated DNA was on average only 3.5%, with a very small standard error (Fig. 2b, “same band”), indicating that our algorithm is valid.

3. Discussion

Here we study the interactions between DNA and gold nanoparticles. We find that heating a DNA-nanoparticles solution results in DNA degradation. Remarkably, the presence of matching short oligonucleotides (22 base pairs) rescues the long DNA plasmids (over 2000 base pairs). We used this phenomenon to successfully detect single nucleotide mutations including two of the most common mutations leading to Cystic Fibrosis. Several methods use nanoparticles to detect mutations [13–18]. Essentially, nanoparticles carry a negative charge preventing aggregation. High concentrations of salt or low pH mask the charge, thereby causing nanoparticle aggregation, resulting in a colorimetric change. In these methods the oligonucleotides are attached to the nanoparticles and mixed with a target DNA. If the DNA matches the oligonucleotides, it hybridizes with the oligonucleotides and aggregation is prevented. If the target DNA is mutated, binding is less efficient and nanoparticle aggregation occurs. In our approach the nanoparticles and the oligonucleotides are not attached.

A possible mechanism to explain our results is based on the previous finding that single stranded (ss) DNA attaches to nanoparticles with a much higher affinity compared to double stranded (ds) DNA [14]. dsDNA is restricted to a double helix structure with negatively charged phosphate groups exposed on the surface, and is repulsed by the negative nanoparticles. In ssDNA, the negative charge on the backbone is sufficiently distant to cause it to stick to the nanoparticles. In our setup, it is plausible that there is competition between binding of oligonucleotides-nanoparticles, and plasmid-nanoparticles (plasmid is naturally ds but becomes ss during heating). If the oligonucleotides match the plasmid, they bind each other and not the nanoparticles, and the plasmid remains intact. If the oligonucleotides do not fully match the plasmid, the denatured plasmid can adsorb to the nanoparticles degrade.

The novel phenomenon we have discovered has applicable aspects for detection of known mutations, i.e. each sample should be tested with a matching and unmatching oligo, and compared to known WT and sick controls. Therefore, this method has the potential to be adapted for future diagnostic applications.

4. Methods

4.1. Nanoparticles

The gold nanoparticles used were NexusBeads™, 5 nm diameter, coated with neutravidin, purchased from BBI International (Cardiff, UK). Approximately 10^{13} nanoparticles (5 μ l) were used for each reaction.

4.2. DNA plasmids

pUC19 was purchased from Invitrogen. pCFmut was designed in our lab and synthesized by Hy-labs. The core of the plasmid is pUC57-Amp, and it includes a ~400 nucleotide insert containing two of the most common mutations leading to the disease Cystic Fibrosis. Full sequence is available upon request. The mutations are delF508 (deletion of three base pairs leads to deletion of phenylalanine at codon 508), and H1282X (G-to-A change in nucleotide 3978 that is responsible for a stop mutation in codon 1282). Our pCFmut plasmid contains the mutated alleles, not the WT. 2 µg of DNA was used for each reaction.

4.3. Oligonucleotides

DNA oligonucleotides were synthesized by Hy-labs. Fig. 1: oligo 9 is the commercial T7 oligo, and does not match the DNA plasmid at all. Oligo 35 fully matches the DNA plasmid. Fig. 2: in oligo 36, the first 21 nucleotides match the DNA plasmid, and the last one does not match. Fig. 4: oligos 97 and 98 correspond to the delF508 mutation (97 corresponds to the mutated allele, 98 corresponds to the WT allele). Oligos 107 and 108 correspond to the H1282X mutation (107 corresponds to the mutated allele, 108 corresponds to the WT allele). 30 pmol of oligonucleotide were used for each reaction.

4.4. Oligonucleotide sequences

Oligo number	Oligo sequence
9	5'-TAATACGACTCACTATAGGG-3'
35	5'-CAGGAAACAGCTATGACCATGA-3'
36	5'-CAGGAAACAGCTATGACCATGT-3'
97	5'-AAATATCATCGGTGTTTCCTAT-3'
98	5'-AATATCATCTTTGGTGTTCCT-3'
107	5'-AAGGAAAGCCTTTGGAGTGATA-3'
108	5'-GAGGAAAGCCTTTGGAGTGATA-3'

4.5. DNA cleanup kit

In order to remove the nanoparticles from the mixture before running the plasmid in an agarose gel, the “Wizard® SV Gel and PCR Clean-Up System” (Promega) was used. This step was critical, since the nanoparticles carry a net negative charge and therefore tend to run in agarose gels in the same direction as DNA, and mask the DNA.

4.6. Gel separation

Separation of the DNA was done using 1% agarose gel, for 30 min at 100 V. Staining was done with ethidium bromide.

4.7. Densitometry and band quantification

Densitometry was done using imageJ software. For band quantification in Fig. 4, our processing algorithm is based on comparing the histograms of the various images obtained from running our DNA through the gel. Each column in the experimentally obtained images is treated as 1-D signal. For each such signal the spectrogram is computed as follows:

$$\begin{aligned} \text{Spectrogram}[m, k] &= \text{SG}[m, k] = \left| \text{DSTFT}[m, k] \right|^2 \\ &= \left| \sum_n s[n]w[n-m] \exp\left(\frac{-2\pi i k n}{N}\right) \right|^2 \end{aligned} \quad (1)$$

where DSTFT is the discrete short time Fourier transform, $s[n]$ is our signal, and $w[n]$ is the sliding window applying the Fourier transform each time on another segment of the inspected 1-D signal $s[n]$. N is the number of pixels in the inspected 1-D signal $s[n]$.

After computing the histograms of the various signals we subtract their DC component, normalize their energy, and compare them by computing the correlation coefficient that is defined as:

$$\begin{aligned} C_{\text{SG}_1, \text{SG}_2} &= \sum_m \sum_k \left(\frac{\text{SG}_1[m, k] - \overline{\text{SG}_1}}{\sqrt{E_{\text{SG}_1}}} \right) \left(\frac{\text{SG}_2[m, k] - \overline{\text{SG}_2}}{\sqrt{E_{\text{SG}_2}}} \right)^* \\ E_{\text{SG}_j} &= \sum_m \sum_k \left| \text{SG}_j[m, k] - \overline{\text{SG}_j} \right|^2 \quad j = 1, 2 \end{aligned} \quad (2)$$

$$\overline{\text{SG}_j} = \sum_m \sum_k \text{SG}_j[m, k] \quad j = 1, 2$$

where E_{SG_j} is the normalizing energy for spectrogram SG_j and is its DC. $C_{\text{SG}_1, \text{SG}_2}$ is the correlation coefficient obtained when comparing spectrogram SG_1 with spectrogram SG_2 . Due to the energy normalization auto correlation coefficient (comparison of the spectrogram with itself) will give the value of 1 (100%), while cross comparison should give lower values. In the spectrogram we enhanced the band pass frequencies while attenuated the low frequencies of the signal.

Acknowledgements

The authors thank Dr. Gal Yerushalmi for help designing Fig. 3. Pazit Polak acknowledges the Israeli Ministry of Immigrant Absorption for financial support.

References

- [1] Q. Wang, L. Yang, X. Yang, K. Wang, L. He, J. Zhu, *Analytica Chimica Acta* 688 (2011) 163–167.
- [2] E.-O. Ganbold, T. Kang, K. Lee, S.Y. Lee, S.-W. Joo, *Colloids and Surfaces B: Biointerfaces* 93 (2011) 148–153.
- [3] C. Shi, Y. Ge, H. Gu, C. Ma, *Biosensors and Bioelectronics* 26 (2011) 4697–4701.
- [4] A.A. Rowe, K.N. Chuh, A.A. Lubin, E.A. Miller, B. Cook, D. Hollis, K.W. Plaxco, *Analytical Chemistry* 83 (2011) 9462–9466.
- [5] M.A. Vlachou, K.M. Glynou, P.C. Ioannou, T.K. Christopoulos, G. Vartholomatos, *Biosensors and Bioelectronics* 26 (2010) 228–234.
- [6] S.I. Stoeva, J.-S. Lee, C.S. Thaxton, C.A. Mirkin, *Angewandte Chemie International Edition* 45 (2006) 3303–3306.
- [7] J.-H. Oh, J.-S. Lee, *Analytical Chemistry* 83 (2011) 7364–7370.
- [8] C.S. Thaxton, D.G. Georganopolou, C.A. Mirkin, *Clinica Chimica Acta* 363 (2006) 120–126.
- [9] O. Salata, *Journal of Nanobiotechnology* 2 (2004) 3.
- [10] R. Mahtab, J.P. Rogers, C.J. Murphy, *Journal of the American Chemical Society* 117 (1995) 9099–9100.
- [11] L. Zhang, F.X. Gu, J.M. Chan, A.Z. Wang, R.S. Langer, O.C. Farokhzad, *Clinical Pharmacology and Therapeutics* 83 (2008) 761–769.
- [12] A.R. Herdt, S.M. Drawz, Y. Kang, T.A. Taton, *Colloids and Surfaces B: Biointerfaces* 51 (2006) 130–139.
- [13] K. Sato, K. Hosokawa, M. Maeda, *Nucleic Acids Research* 33 (2005) e4.
- [14] H. Li, L. Rothberg, *Proceedings of the National Academy of Sciences of the United States of America* 101 (2004) 14036–14039.
- [15] G. Doria, R. Franco, P. Baptista, *IET Nanobiotechnology* 1 (2007) 53–57.
- [16] W.J. Qin, O.S. Yim, P.S. Lai, L.-Y.L. Yung, *Biosensors and Bioelectronics* 25 (2010) 2021–2025.
- [17] L. Sun, Z. Zhang, S. Wang, J. Zhang, H. Li, L. Ren, J. Weng, Q. Zhang, *Nanoscale Research Letters* 4 (2008) 216–220.
- [18] Z. Zhan, X. Ma, C. Cao, S.J. Sim, *Biosensors and Bioelectronics* 32 (2012) 127–132.